

Language organization and temporal correlations in the spiking activity of an excitable laser: Experiments and model comparison

Nicolas Rubido,¹ Jordi Tiana-Alsina,² M. C. Torrent,² Jordi Garcia-Ojalvo,² and Cristina Masoller²

¹*Facultad de Ciencias, Instituto de Física, Universidad de la República, Iguá 4225, Montevideo, Uruguay*

²*Departament de Física i Enginyeria Nuclear, Universitat Politècnica de Catalunya, 08222 Terrassa, Barcelona, Spain*

(Received 4 May 2011; revised manuscript received 4 July 2011; published 9 August 2011)

We introduce a method, based on symbolic analysis, to characterize the temporal correlations of the spiking activity exhibited by excitable systems. The technique is applied to the experimentally observed dynamics of a semiconductor laser with optical feedback operating in the low-frequency fluctuations regime, where the laser intensity displays irregular trains of sudden dropouts that can be interpreted as excitable pulses. Symbolic analysis transforms the series of interdropout time intervals into sequences of words, which represent the local ordering of a certain (small) number of those intervals. We then focus on the transition probabilities between pairs of words, showing that certain transitions are overrepresented (resulting in others being underrepresented) with respect to the surrogate series, provided the laser injection current is above a critical value. These experimental observations are in very good agreement with numerical simulations of the delay-differential Lang-Kobayashi model that is commonly used to describe this laser system, which supports the fact that the language organization reported here is generic and not a particular feature of the specific laser employed or the experimental time series analyzed. We also present results of simulations of the phenomenological nondelayed Eguia-Mindlin-Giudici(EMG) model and find that in this model the agreement between the experiments and the simulations is good at a qualitative, but not at a quantitative, level.

DOI: [10.1103/PhysRevE.84.026202](https://doi.org/10.1103/PhysRevE.84.026202)

PACS number(s): 05.45.-a, 42.60.Mi, 42.55.Px, 42.65.Sf

I. INTRODUCTION

The specific subthreshold dynamics of an excitable system determines the correlation statistics of the pulse trains that it generates [1]. These correlations in turn affect the functionality of the system by regulating, for instance, its information encoding capabilities [2,3]. It is thus important to establish the temporal organization of the spiking activity displayed by excitable systems. In this paper we present a method to characterize this temporal organization based on symbolic analysis of the series of interspike time intervals. The method is applied to the experimental time series generated by an excitable system, namely, a semiconductor laser with optical feedback.

When operating near the laser threshold and for moderate feedback levels, semiconductor lasers with optical feedback exhibit a regime of low-frequency fluctuations (LFFs), consisting in sudden intensity dropouts followed by gradual stepwise recoveries [4–6]. In the LFF regime, the laser responds as an excitable system [7–9] with a dynamics that resembles neuronal behavior. Much effort has been devoted to the understanding and characterization of the excitable nature of the intensity power dropouts. In particular, an issue that has attracted much attention is the relative influence of the stochastic and deterministic nonlinear processes that are responsible for the dropouts. Several authors have investigated the characteristics of the LFFs in terms of the statistics of both the intensity fluctuations [10–12] and the time intervals between consecutive dropouts [9,13–17] (in particular their probability distribution function), which are equivalent to the interspike intervals in neurons.

As the laser bias current is increased above threshold, the intensity dropouts become more frequent and begin to merge and eventually the laser output displays a sequence of erratic fluctuations, a regime that has been called coherence collapse

(CC). This regime has been identified as a high-dimensional chaotic dynamics [18], the high dimensionality resulting from the delay time associated with optical feedback due to the finite flight time of the light in the external cavity. The CC regime has been studied in the past by employing well-known techniques such as those based on Poincaré sections, Lyapunov exponents, and fractal dimensions [18–20].

Recently, attention has focused on studying the degree of complexity of the laser dynamics by employing alternative methodologies of nonlinear symbolic time-series analysis. In particular, we recently applied the so-called ordinal pattern methodology to investigate the gradual change in the dynamics that takes place during the transition from LFFs to coherence collapse when the laser bias current increases [21].

The ordinal pattern methodology is based on defining patterns (or “words”) in a time series that result from ordering relations in sets of consecutive values of the series [22,23]. After computing the probabilities of the various patterns, one can characterize the dynamics of the system by means of information-theory measures such as the Shannon entropy and the Martin-Plastino-Rosso (MPR) statistical complexity [24]. These two measures showed that during the transition from the LFF to the CC regime the entropy first diminished and then saturated, while the statistical complexity first increased and then saturated [21].

In this paper we aim to go beyond the analysis of Ref. [21] in two ways. First, we calculate the probabilities of transitions between consecutive ordinal patterns [25]. In other words, we analyze the “language” of the LFFs by detecting consecutive words that appear with high relative frequency, similar to the sequences of words “it is” and “they are,” which are quite common in the English language. Second, this analysis in turn provides us with the opportunity to perform a detailed comparison between experiments and theory.

Our results show that close to coherence collapse (but still in the LFF regime) not all the transition probabilities are equally probable; there are a few of them significantly more probable than the rest, which we consider to be a signature of deterministic triggering mechanisms. In contrast, closer to threshold all the transition probabilities are similar, which suggests that in this region the LFFs are mainly triggered by noise. This result is coherent with previous reports in the literature for both single lasers with optical feedback [11,26] and coupled lasers [27].

We critically compare the experimental results with model predictions. Several models have been proposed in the literature to explain the LFF dynamics [8,28–30]. A well known model is the Lang-Kobayashi (LK) model [31], which consists of a set of delay-differential rate equations for the complex laser field and the carrier density. The LK model has been shown to successfully describe many features of the LFFs [12,19,32–34]. A phenomenological model, proposed by Eguia, Mindlin, and Giudici [8], consists of a set of ordinary differential equations and also has been shown to explain many features of the LFFs [14,35,36].

We compare the predictions of these two models and find that the experimental observations are in good agreement with simulations of the LK model; in particular, the word that is significantly more probable in the LK simulations is the same as in the experiments. In contrast, the agreement with simulations of the Eguia-Mindlin-Giudici (EMG) model is only qualitative, as in simulations of this model the most significant word is not the same as in the experiments. Thus we show that the ordinal pattern method can also be used to distinguish among numerical models.

This paper is organized as follows. The experimental system is introduced in Sec. II, where we also present the ordinal pattern method and the definition of the transition probabilities (TPs). In Sec. III we present the results of the analysis of the experimental time series of interdropout intervals (IDIs). The analysis clearly reveals that, for pump currents close to coherence collapse, there are temporal correlations in the IDIs time series that result in some transition probabilities being significantly more probable than the rest. In Sec. IV we present results of the analysis of simulations of the LK model [31] and the EMG model [8]. Our conclusions are presented in Sec. V.

II. EXPERIMENTAL SYSTEM AND SYMBOLIC METHODOLOGY

A. Experimental setup

Our excitable system consists of an AlGaInP Fabry-Pérot semiconductor laser (Sharp GH06510B2A) with a nominal wavelength $\lambda_n = 650$ nm, subject to optical feedback from an external mirror. Details of the experimental setup can be found in Ref. [21]. The laser output was measured for increasing bias current, which leads to an increase in the frequency of the power dropouts. A typical time trace of the laser output is shown in Fig. 1(a), where intensity dropouts are clearly seen [Fig. 1(b) displays power dropouts simulated from the LK model and will be discussed in detail in Sec. IV A].

The dropouts start to merge for large enough pump current, thus leading to the qualitatively different dynamical behavior

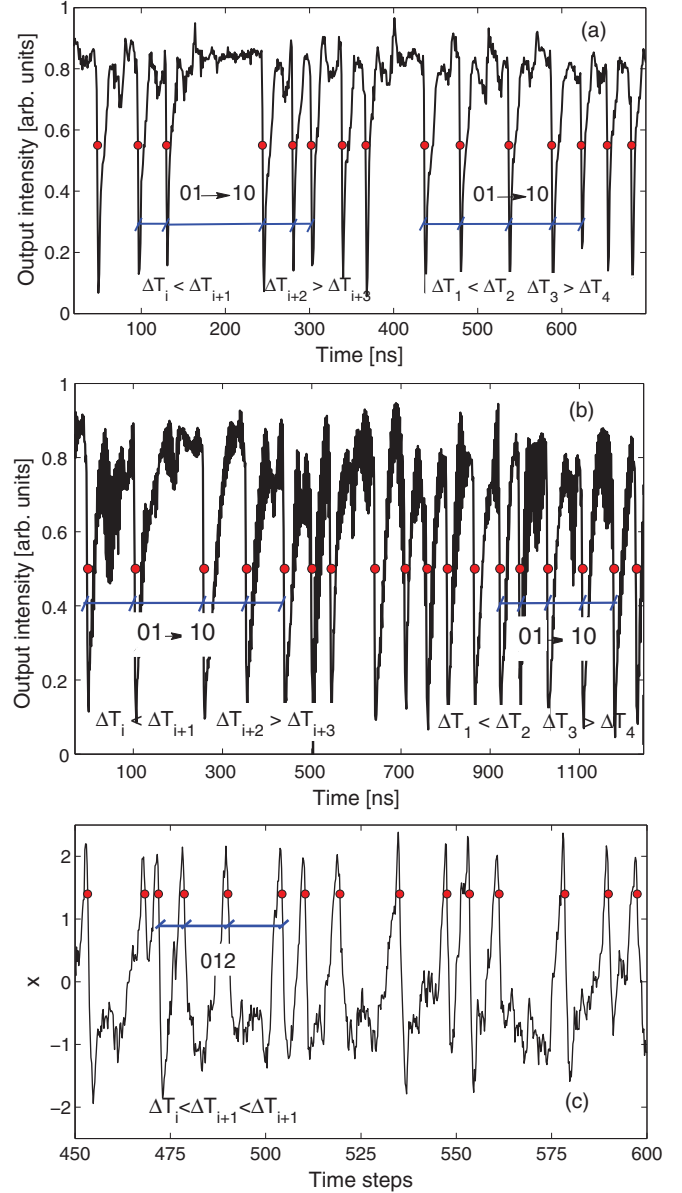


FIG. 1. (Color online) (a) Experimental time series of the laser intensity for an injection current $I = 34$ mA, (b) simulated intensity from the LK model with a pump current parameter $\mu = 1.08$ (see Sec. IV A for details), and (c) simulated time trace from the EMG model with $\beta = 0.1$, $\epsilon_1 = 0.26$, and $\epsilon_2 = 0.44$ (see Sec. IV B for details). The circles indicate the times used to calculate the interdropout intervals; a few words and transitions are indicated as examples.

of coherence collapse. Previous work [21] characterized this transition in terms of complexity measures applied to the time series of the IDIs. The results showed that the normalized Shannon entropy was close to 1 all the way up to a critical pump current, which we will refer to as I_c ($I_c \simeq 33$ mA), after which it leveled off rapidly at a value smaller than 1.

B. Ordinal patterns and transition probabilities

In order to further characterize these variations in the dynamical behavior of the LFFs, we transform the time series

of IDIs $\{\Delta T_0, \Delta T_1, \Delta T_2, \dots\}$ into a series of words or ordinal patterns (OPs) $\{s_1, s_2, \dots\}$ following the Bandt-Pompe (BP) method [22,23]. We present here a discussion of the main ideas of the method.

The first step is to divide a time series $\{x(t), t = 1, \dots, M\}$ into $M - D$ overlapping vectors of dimension D . Then each element of a vector is replaced by a number from zero to $D - 1$, in accordance with the relative strength of the element in the ordered sequence (with zero corresponding to the shortest and $D - 1$ to the longest value in each vector). Each vector then has associated an ordinal pattern composed of D symbols. For example, with $D = 3$, the IDI sequence $\{\Delta T_0, \Delta T_1, \Delta T_2\} = \{5, 1, 10\}$ gives the ordinal pattern (1 0 2) as $\Delta T_1 < \Delta T_0 < \Delta T_2$.

The number of different ordinal patterns of dimension D is $D!$. By counting the number of times a pattern s_i appears in the sequence $\{s_1, s_2, \dots\}$ one can compute the probability distribution functions (PDFs) of the ordinal patterns. Since the number of possible ordinal patterns is $D!$, to have a good statistics one must have a long enough time series such that $(M - D) \gg D!$.

In the following we consider various pattern lengths, specifically, $D = 2, 3$, and 4, and compute the PDFs of the $D!$ possible patterns and the $D! \times D!$ TPs between these patterns [25]. The TPs quantify the frequency at which a certain pattern in the time series transforms into another one and constitute an alternative way to yield insight into time correlations present in the laser dynamics.

The ordinal patterns can be labeled, without loss of generality, by means of a scalar $\alpha = 1, \dots, D!$ with increasing values according to their degree of increase between consecutive IDIs. For instance, in the case $D = 2$, the order relation $\Delta T_m \geq \Delta T_{m+1}$ for the m th and $(m + 1)$ th IDIs of the series (“10” in the BP notation) corresponds to $\alpha = 1$, while $\alpha = 2$ denotes the pattern $\Delta T_m < \Delta T_{m+1}$ (“01” in the BP notation) (see Fig. 1); in the case $D = 3$, $\alpha = 1$ represents the “210” pattern ($\Delta T_m \geq \Delta T_{m+1} \geq \Delta T_{m+2}$), $\alpha = 2$ stands for the “201” pattern ($\Delta T_m \geq \Delta T_{m+2} > \Delta T_{m+1}$), and so on. Using this notation, the TPs can be expressed as $P(\alpha \rightarrow \beta)$, where α and β can take any value of the set $\{1, \dots, D!\}$, and

$$P(\alpha \rightarrow \beta) = \frac{\sum_{t=1}^L n(s_t = \alpha, s_{t+1} = \beta)}{\sum_{t=1}^L n(s_t = \alpha)}, \quad (1)$$

where n is a count of the number of times of occurrence in the series of OPs, $\{s_1, s_2, \dots, s_L\}$, of length L .

Only nonoverlapping words are considered in what follows. Hence, for M IDIs, the number of patterns generated is $L = \lfloor (M - D)/D \rfloor + 1$, where $\lfloor x \rfloor$ denotes the largest integer less than or equal to x . Under these conditions, for surrogated data all TPs are expected to be equal to $1/D!$, corresponding to a Markov process between word pairs. In order to have good statistics the number of OPs must be much larger than the number of possible transitions, i.e., $(M - D)/D \gg D! \times D!$. In the following section the analysis is done with time series of $M \simeq 10^4$ IDIs, which results in sequences of about 3300 (5000) words of $D = 3$ ($D = 2$).

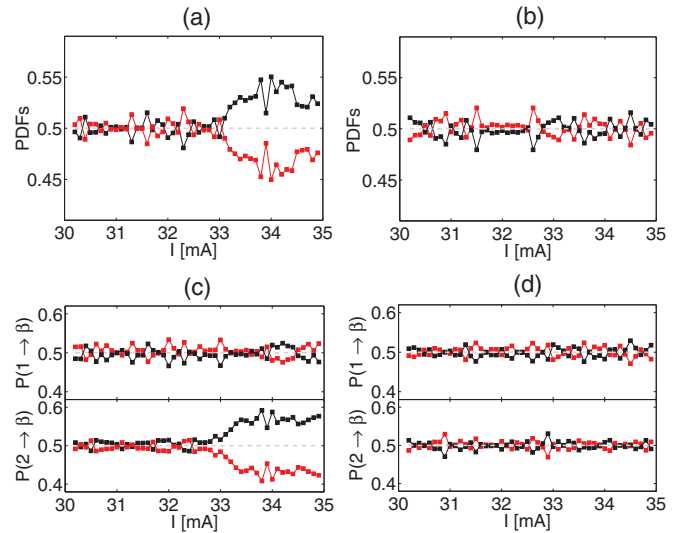


FIG. 2. (Color online) (a) and (b) Probability distributions of the two possible words for $D = 2$ [$\alpha = 1$ is shown in black and $\alpha = 2$ in gray (red online)] and (c) and (d) the four possible transition probabilities between consecutive words (colors corresponds to the transitioned word) vs the laser injection current. Results are displayed for (a) and (c) the experimental time series and (b) and (d) the surrogated data. The dashed horizontal gray lines indicate the equally distributed probabilities that are expected for random series.

III. EXPERIMENTAL RESULTS

A typical example of the word transitions discussed above is displayed in Fig. 1, where two instances of the transition from the word $\alpha = 2$ (“01”) to the word $\beta = 1$ (“10”) can be seen.

In the experimental time series [Fig. 1(a)] this is a typical situation: When the pump current is greater than the critical pump current $I_c \simeq 33$ mA, the transition from word $\alpha = 2$ to word $\beta = 1$ is overrepresented in the laser language [for comparison, Fig. 1(b) displays numerical results, which will be discussed in Sec. IV A].

This can be clearly seen in Fig. 2, which plots the PDFs of the two words [Figs. 2(a) and 2(d)] and the probabilities of the four transitions between them [Figs. 2(c) and 2(d)]. The figure compares the results obtained from analyzing both the experimental time series [Figs. 2(a) and 2(c)] and the surrogated time series [Figs. 2(b) and 2(d)].

Figure 2(a) reveals that for $D = 2$ the two words (“01” and “10”) are equally represented in the experimental time series up to the critical current value $I_c \simeq 33$ mA, beyond which one of the words (“10,” $\alpha = 1$) becomes overrepresented at the expense of the other (“01,” $\alpha = 2$). This behavior is related to the changes in the statistical complexity that were observed in Ref. [21] at the same pump current.

We note that this behavior is robust and does not depend on where in the IDI series the word encoding begins. This contrasts with the case of a regular periodic series: For a repetitive set of words $\alpha = 2$ (“01”), for instance, a shift of one position in the IDI series would transform all the words into $\alpha = 1$ (“10”). The fact that this does not happen in our case highlights the irregular character of our series, in spite of which a clear overrepresentation of a word emerges for large

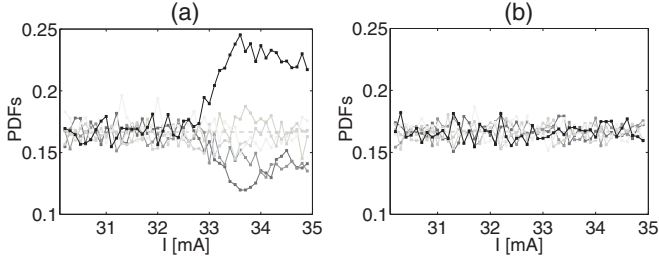


FIG. 3. Probability distributions of the six words with $D = 3$ vs the pump current for both (a) the experimental and (b) the surrogated time series. The different words are represented in grayscale, with black corresponding to $\alpha = 1$ and lighter grays to α increasing up to 6.

enough pump current. Note that in Fig. 2(a) the two PDFs level off shortly after I_c . This phenomenon is conspicuously absent for the surrogated series [Fig. 2(b)].

Concurrently with the changes exhibited by the word PDFs as the pump current increases, a similar behavior occurs for the transition probabilities. In particular, starting again at $I_c = 33$ mA, the transition from $\alpha = 2$ to $\beta = 1$ becomes clearly overrepresented, in this case at the expense of the $2 \rightarrow 2$ transition, as shown in Fig. 2(c). Transitions departing from $\alpha = 1$ are left unchanged throughout all pump levels. Once again, the phenomenon is, as expected, absent in the surrogated series [Fig. 2(d)].

The results presented above for $D = 2$ (two-letter words) are also seen for three-letter words $D = 3$. For instance, regarding the relative frequencies of the six words that exist for $D = 3$, once more all words are equally probable for low enough pump currents [Fig. 3(a)]. However, for currents above the critical value one of the words ($\alpha = 1$, namely, “210”) becomes overrepresented, at the expense mainly of $\alpha = 2$ (“201”), which becomes less frequent than the average, also in comparison with the surrogate [Fig. 3(b)]. In general, the results reveal a large heterogeneity in the relative frequencies of the different words for $I > I_c$, with several words departing from the equidistribution value, either above or below it and in different amounts.

The most frequent word $\alpha = 1$ appears to be also the most frequently transitioned to, as shown in Fig. 4. Correspondingly, the least frequent word $\alpha = 2$ is also the one least frequently transitioned to. Therefore, decreasing patterns seem to be the predominant ones when the pump current is above the critical value. These conclusions also hold for words of four letters, where “3210” appears to be the most recurrent pattern beyond I_c [however, the differences among the probabilities of the different words are less pronounced (the results are not shown)].

In order to make the heterogeneity of the word PDFs and TPs reported above more evident, in Fig. 5 we compare, for $D = 3$, the PDFs of the 6 possible words [Figs. 5(a) and 5(c)] and the 36 TPs [Figs. 5(b) and 5(d)] for two different injection currents: below the critical current value I_c [Figs. 5(a) and 5(b)] and above the critical current value I_c [Figs. 5(c) and 5(d)]. In all the panels, the black bars correspond to the experimental series and the red bars (gray online) correspond to the surrogated series.

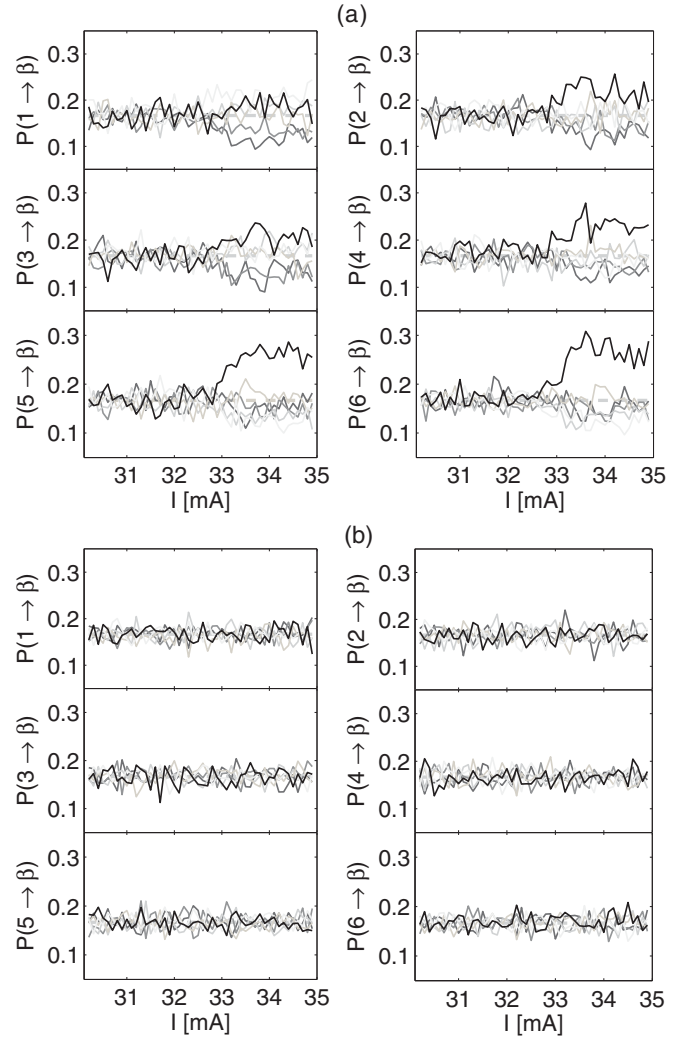


FIG. 4. Transition probabilities vs pump current for the 36 possible transitions between consecutive words with $D = 3$. The plots are organized according to the starting word, with the final word represented in grayscale, following the criterion of Fig. 3. Also shown are results for (a) the experimental series and (b) the surrogate series.

One can notice that in the panel corresponding to $I > I_c$ the word distribution shows a behavior that is clearly different from that of the surrogate data [Fig. 5(c)], while these differences disappear when the pump current is smaller than I_c [Fig. 5(a)]. The TPs are more heterogeneous above the critical current, in comparison with surrogate data [Fig. 5(d)], than below the critical current [Fig. 5(b)].

So far we have analyzed transitions probabilities between consecutive words, but there could be higher-order correlations in the word transitions. An inspection of Figs. 2(a) and 2(c) reveals that, for $I > I_c$, differences for the TPs are higher than for the PDFs. For instance, for $I = 34$ mA, the underrepresented and overrepresented TPs are close to 0.4 and 0.6, respectively, whereas the PDFs are close to 0.45 and 0.55. In other words, the TPs exhibit asymmetries larger than the word’s PDFs.

In order to see how long lasting these high-order correlations are, we performed a statistical analysis of the

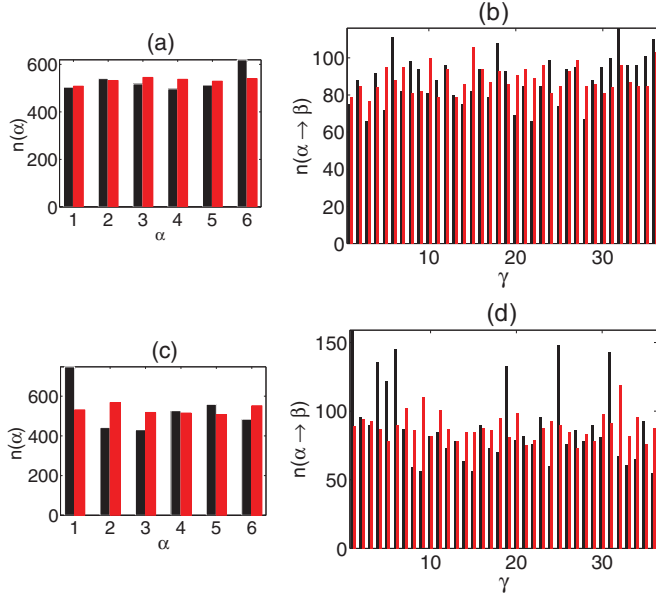


FIG. 5. (Color online) Histograms of the occurrences of (a) and (c) words of $D = 3$ and (b) and (d) consecutive transitions at a pump current (a) and (b) below the critical value $I = 32$ mA and (c) and (d) above the critical value $I = 34$ mA. The numbers of transition are labeled from $\alpha = 1 \rightarrow \beta = 1$ ($\gamma = 1$) to $\alpha = 6 \rightarrow \beta = 6$ ($\gamma = 36$). Black bars correspond to the experimental series and the gray bars (red online) correspond to the surrogated series.

transitions between nonconsecutive words. Figure 6 shows, for a fixed laser current, the probabilities of transitions between increasingly distant patterns,

$$P_{\tau_{\text{lag}}}(\alpha \rightarrow \beta) = \frac{\sum_{t=1}^L n(s_t = \alpha, s_{t+\tau_{\text{lag}}} = \beta)}{\sum_{t=1}^L n(s_t = \alpha)}, \quad (2)$$

where n is the number of occurrences in a series.

Figure 6 shows that as transitions between more distant words are considered, i.e., as τ_{lag} increases, word correlations are lost and the TPs end up exhibiting the statistical nature of the word appearances in the IDI series, as revealed by the PDFs. In other words, the deterministic signature arising for injection currents larger than I_c is lost when transitions

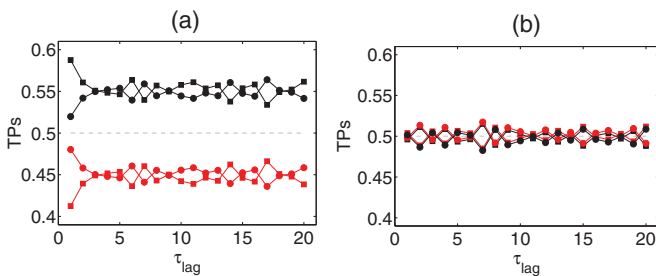


FIG. 6. (Color online) Transition probabilities between words of $D = 2$ separated by τ_{lag} [see Eq. (2)] for an injection current above the critical value $I = 34$ mA. The right column shows the experimental data; the left column shows the surrogate data. Circles correspond to $\alpha = 1$ and squares correspond to $\alpha = 2$. Colors stand for the transitioned pattern: Black is $\beta = 1$ and gray (red online) is $\beta = 2$.

between nonconsecutive patterns separated more than two IDIs are considered.

We note that these observations are robust against experimental parameter variations such as time delay and feedback strength. We performed experiments with different semiconductor lasers and setup arrangements and observed the same results. Specifically, the words “0” for $D = 2$ and “210” for $D = 3$ are overrepresented in the LFF dynamics for current values close to coherence collapse.

We interpret these observations as due to the topology of the phase space of the laser dynamics, which is such that when the dropouts are very frequent, if a dropout occurs before the laser is fully recovered from the previous one, it performs an excursion in phase space that is shorter than the previous one, so that the following interdropout interval will be shorter than the previous one.

IV. MODELS

In order to test whether the above reported observations are particular to the specific experimental conditions used for the generation of the time series, we now turn to numerical modeling. We critically compare the observations with the predictions of two models: the Lang-Kobayashi model [31] and Eguia-Mindlin-Giudici model [8].

A. The Lang-Kobayashi model

The Lang-Kobayashi delay-differential equations describing a single-mode semiconductor laser with optical feedback are [31]

$$\frac{dE}{dt} = k(1 + i\alpha)[g(N, |E|^2) - 1]E + \eta E(t - \tau)e^{-i\omega_0\tau} + \sqrt{\beta_{\text{sp}}}\xi(t), \quad (3)$$

$$\frac{dN}{dt} = \gamma_N(\mu - N - g|E|^2), \quad (4)$$

where E is the slowly varying complex field amplitude, N is the carrier density, and g is the optical gain that includes a saturation coefficient ϵ , $g(N, |E|^2) = N/(1 + \epsilon|E|^2)$. Other internal parameters of the laser are the field decay rate k , the carrier decay rate γ_N , the linewidth enhancement factor α , the noise strength β_{sp} , and the injection current parameter μ , normalized such that the threshold of the solitary laser is at $\mu_{\text{th}} = 1$. Additionally, $\xi(t)$ is a Gaussian white noise of zero mean and intensity unity. The optical feedback parameters are η , τ , and $\omega_0\tau$, which represent the feedback strength, delay time, and feedback phase, respectively (ω_0 is the emission frequency of the solitary laser in the absence of optical feedback).

Close to threshold and under moderately strong feedback, the laser intensity displays fast picosecond pulses. When the intensity time series is filtered (with a filter that simulates the finite bandwidth of the experimental detectors) power dropouts are observed, such as those displayed in Fig. 1(b), which are very similar to the ones seen experimentally. This figure already suggests that $\alpha = 1$ is a frequent word and that the interword transition going from $\alpha = 2$ to $\beta = 1$ is also frequent, in good agreement with the experimental results. In

order to verify this observation, we now perform systematic numerical simulations to quantify the corresponding PDFs and TPs with good statistics.

The parameters used in the simulations are $k = 300 \text{ ns}^{-1}$, $\alpha = 4$, $\gamma_N = 1 \text{ ns}^{-1}$, $\epsilon = 0.01$, $\beta_{\text{sp}} = 10^{-4} \text{ ns}^{-1}$, $\eta = 60 \text{ ns}^{-1}$, and $\tau = 3 \text{ ns}$, while μ is varied. For these parameters we have (except when μ is close to the threshold) a large number of power dropouts before the LFFs die away [12,37]. This allows us to compute the word PDFs with good statistics. When the pump current parameter is close to threshold, the transient LFF dynamics is short and there are not enough dropouts to compute the word statistics reliably. To overcome this problem we simulated several stochastic trajectories, with both different noise realizations in the rate equations and different stochastic initial conditions, which were chosen with the optical field at the noise level, $E(t) = \xi(t)$, $0 \leq t \leq \tau$, and $N(0) = 0$.

Numerical simulations of the LK model with the parameters given in the preceding paragraph lead to trains of intensity dropouts, an example of which is shown in Fig. 1(b), discussed above. The PDFs of the words resulting from these IDI series, and the corresponding TPs, are shown for increasing pump currents in Fig. 7. The results show qualitative agreement with Fig. 2: As the pump current increases, the frequency of the word $\alpha = 1$ (“10”) grows and the transition from $\alpha = 2$ to $\beta = 1$ (i.e., from “01” to “10”) becomes more probable.

The results for $D = 3$ (Fig. 8) show the same qualitative agreement with the experiments as for $D = 2$. In particular, for $D = 3$ the word $\alpha = 1$ (“210”) is the most probable to occur and to be transitioned to. The agreement also holds for the least likely word ($\alpha = 2$, i.e., “201”), as can be seen in Fig. 8(a).

We note that for both $D = 2$ and $D = 3$, the agreement between theory and experiments is remarkable, as the preferred word and transition are the same here as in the experimental

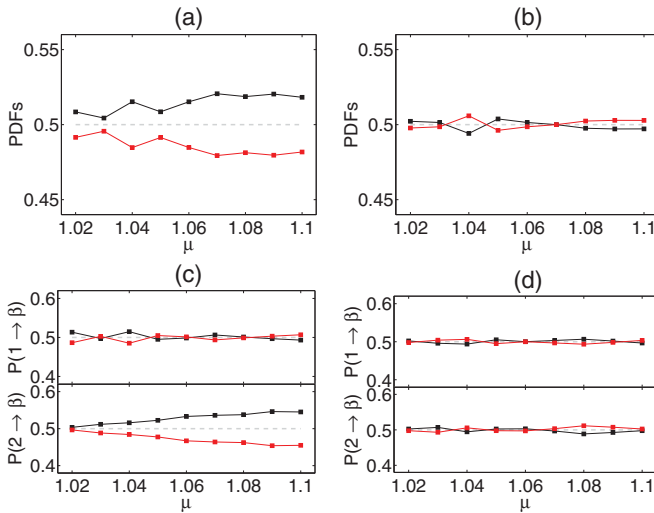


FIG. 7. (Color online) Results of simulations of the LK model. Words with $D = 2$ are considered. PDFs of the two possible words vs the pump current parameter, computed from (a) the numerical time series and (b) their surrogates, are shown. Also depicted are the corresponding TPs between consecutive words, again for (c) the numerical series and (d) their surrogates. The color coding is the same as in Fig. 2.

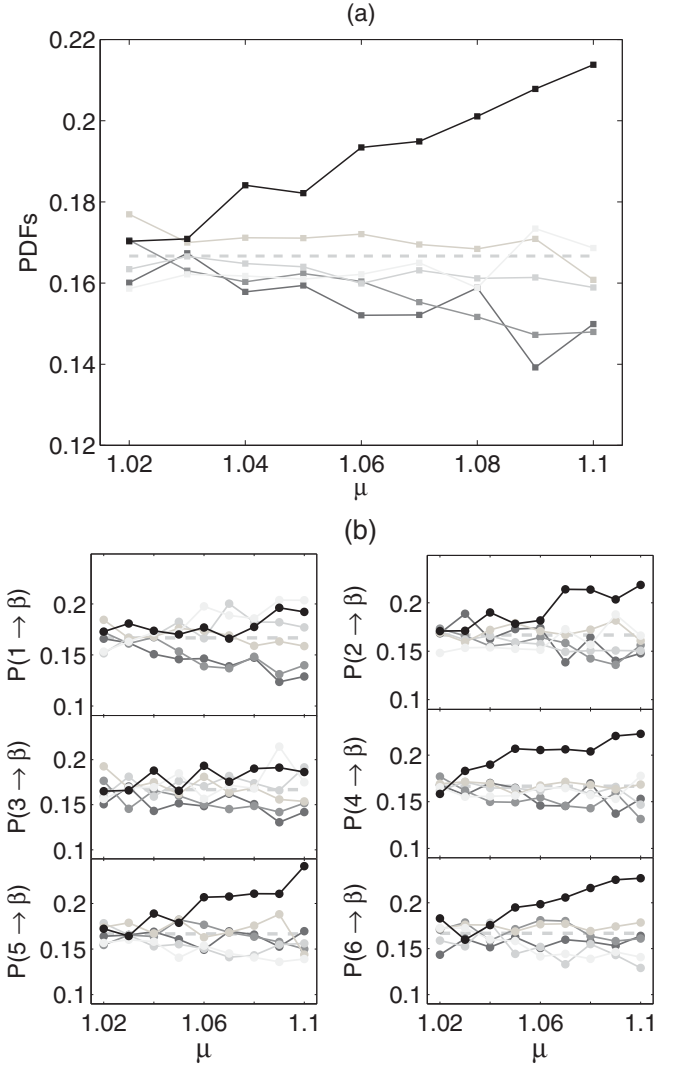


FIG. 8. Results of simulations of the LK model, considering words with $D = 3$. PDFs of the six possible words vs the pump current, computed from (a) the numerically generated time series and (b) the corresponding TPs between consecutive words. The color coding is the same as in Fig. 3.

time series. This result is relevant because it demonstrates that the behavior is a general feature of semiconductor lasers with optical feedback and not of the specific device and/or conditions of this experiment.

B. The EMG model

The rate equations of the phenomenological, low-dimensional model proposed by Eguia *et al.* are [8]

$$\frac{dx}{dt} = y + \sqrt{2\beta}\xi(t), \quad (5)$$

$$\frac{dy}{dt} = x - y - x^3 + xy + \epsilon_1 + \epsilon_2 x^2, \quad (6)$$

where ϵ_1 and ϵ_2 are control parameters, β is the noise strength and $\xi(t)$ is a Gaussian white noise.

The model exhibits excitability for appropriate parameters [38]. In the excitable regime the model has three fixed points:

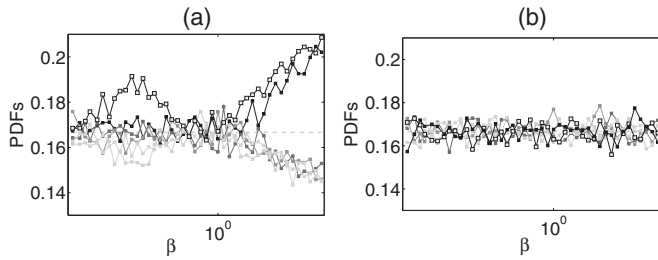


FIG. 9. Results of simulations of the EMG model, considering words with $D = 3$. The PDFs of the six possible words are plotted vs the noise strength (in arbitrary units) for (a) the original data and (b) the surrogated data. The color coding is the same as in Fig. 3, except the word “012” ($\alpha = 6$), which now is represented, for clarity, with a black line and open squares. The parameters are the same as in Fig. 1(c).

a stable focus (node), a saddle point, and an unstable focus (repeller). An initial condition close to the node, in the presence of noise, may result in a trajectory that crosses the stable manifold of the saddle and relaxes back after a long excursion in phase space. These pulses can be associated with the dropouts of the laser intensity in the LFF dynamics. The noise term makes the LFFs sustained in time. A typical time series displaying such noise-induced pulses was presented in Fig. 1(c).

We computed the PDFs of the ordinal patterns and the corresponding TPs for parameters within the excitable region when the amount of noise was varied. The results are presented in Figs. 9 (PDFs) and 10 (TPs) for the original and the surrogated data. First, one can observe that for low noise strength all words are equally probable (as in the experiments and LK simulations), while for an intermediate amount of noise the word “012” ($\alpha = 6$) shows a higher probability of appearance, which does not occur in either the experiments or the LK simulations. For even higher noise strength, not only the word “012” is overrepresented, but also the word “210” is overrepresented, which also does not fully agree with the experiments and the LK simulations, where only the word “210” is overrepresented.

Therefore, we can conclude that while the EMG model captures many features of the LFFs, the subtle time correlations among a few consecutive dropouts is not fully represented. This can be due to the low dimensionality of the EMG model. The laser with optical feedback is a time-delayed system and in that sense the LK model, which has a delayed term, is more likely to represent the high-dimensional phase space of the experimental system.

Since in the EMG model the parameter ϵ_1 has been associated with the laser bias current [14], we also studied the effect of varying this parameter and did not find an improvement in the agreement with the experimental observations (results not shown). Perhaps in this model, to effectively simulate the variation of the laser current, one needs to simultaneously vary both ϵ_1 and β ; however, this is an interesting study that is beyond of the scope of the present work. Our results also point to the fact that the ordinal pattern methodology can be a powerful tool for determining subtle differences among various numerical models, which cannot be uncovered by other methods that do not take into account the time ordering of the

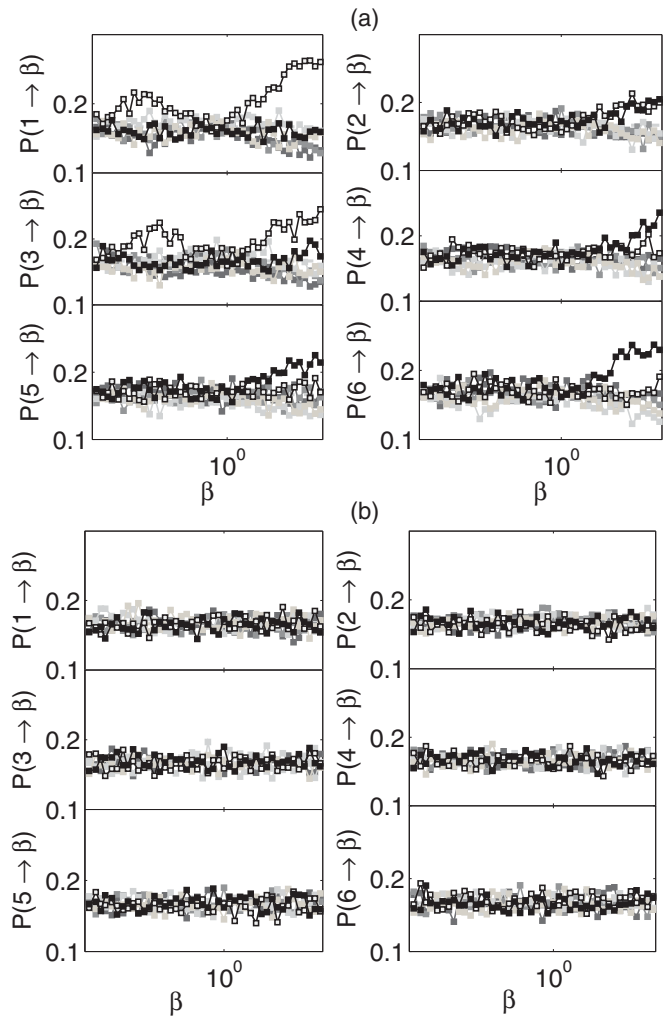


FIG. 10. Transition probabilities vs the noise strength (in arbitrary units) for simulations of the EMG model. The 36 possible transitions between consecutive nonoverlapping words with $D = 3$ are shown. The plots are organized and colored according to the same criteria used in Fig. 4. Also shown are the results of (a) the original time series and (b) the surrogate series. The parameters are the same as those in Fig. 1(c).

sequence of dropout events, such as the study of the interspike time distributions.

V. CONCLUSION

We have characterized experimentally and numerically the language organization of a semiconductor laser with optical feedback operating in an excitable regime. This regime allows us to represent the laser dynamics in terms of a language of words, which represent the ordinal relations within sets of consecutive interevent intervals.

Our results show that at low pump currents all words occur with the same frequency and the same probability to be transitioned to; thus we can interpret that the dropouts are uncorrelated and memory effects play no role and, consequently, that the dropouts are mainly driven by noise. As the injection current increases the dropouts become more frequent and time correlations between them appear. These

correlations imply that there is some memory in the system, so that certain words and transitions become more frequent than others. We conjecture that this behavior is a signature of determinism in the system for sufficiently large pump currents. This result agrees with previous investigations of the same experimental situation via complexity measures [21], but goes beyond that analysis, since the distribution of transition probabilities between words quantifies a higher-order organization of the language. We have also shown that the words lose their correlations when we increase the distance between transitioning words, at which point the TPs match the probability of the word appearance.

We also performed a critical comparison of the observations with the predictions of two models: the Lang-Kobayashi model [31] and the Eguia-Mindlin-Giudici model [8]. The LK model is a time-delayed model (and thus its phase space is infinite dimensional) while the EMG model is a low-dimensional one. We found that in spite of the fact that both models successfully predict the probability distribution of the interdropout intervals, their predictions differ regarding the probability distribution of the ordinal patterns and the transition probabilities.

In the LK model the preferred word and transition are the same as in the experimental time series, which confirms the

generic nature of the experimental observations, independent of the semiconductor laser device and/or the parameters. In the EMG model the agreement is not as good, as not only is the word “210” overrepresented (in good agreement with observations), but so is the word “012,” which is not observed experimentally. Therefore, our results also show that the ordinal pattern methodology can be a powerful tool for determining subtle differences among excitable models that cannot be uncovered by methods that do not take into account the time ordering of the sequence of excitable pulses.

ACKNOWLEDGMENTS

This research was supported in part by the Spanish Ministerio de Ciencia e Innovación through Project No. FIS2009-13360-C03-02, the Air Force Office Scientific Research through Project No. FA-8655-10-1-3075 (C.M.), the Programa I3 (Incentivación de la Incorporación e Intensificación de la Actividad Investigadora, Spain) (J.G.O.), and the Agència de Gestió d’Ajuts Universitaris i de Recerca, Generalitat de Catalunya, through Project No. 2009 SGR 1168. C.M. and J.G.-O. also acknowledge the *foundation* Institució Catalana de Recerca i Estudis Avançats for financial support.

-
- [1] M. J. Chacron, B. Lindner, and A. Longtin, *Phys. Rev. Lett.* **92**, 080601 (2004).
 - [2] M. J. Chacron, A. Longtin, and L. Maler, *J. Neurosci.* **21**, 5328 (2001).
 - [3] O. Avila Akerberg and M. J. Chacron, *Exp. Brain Res.* **210**, 353 (2011).
 - [4] T. Sano, *Phys. Rev. A* **50**, 2719 (1994).
 - [5] I. Fischer, G. H. M. van Tartwijk, A. M. Levine, W. Elsässer, E. Göbel, and D. Lenstra, *Phys. Rev. Lett.* **76**, 220 (1996).
 - [6] G. Vaschenko, M. Giudici, J. J. Rocca, C. S. Menoni, J. R. Tredicce, and S. Balle, *Phys. Rev. Lett.* **81**, 5536 (1998).
 - [7] M. Giudici, C. Green, G. Giacomelli, U. Nespolo, and J. R. Tredicce, *Phys. Rev. E* **55**, 6414 (1997).
 - [8] M. C. Eguia, G. B. Mindlin, and M. Giudici, *Phys. Rev. E* **58**, 2636 (1998).
 - [9] J. Mulet and C. R. Mirasso, *Phys. Rev. E* **59**, 5400 (1999).
 - [10] D. W. Sukow, T. Heil, I. Fischer, A. Gavrielides, A. Hohl-AbiChedid, and W. Elsasser, *Phys. Rev. A* **60**, 667 (1999).
 - [11] J. Hales, A. Zhukov, R. Roy, and M. I. Dykman, *Phys. Rev. Lett.* **85**, 78 (2000).
 - [12] A. Torcini, S. Barland, G. Giacomelli, and F. Marin, *Phys. Rev. A* **74**, 063801 (2006).
 - [13] A. Hohl, H. J. C. van der Linden, and R. Roy, *Opt. Lett.* **20**, 2396 (1995).
 - [14] A. M. Yacomotti, M. C. Eguia, J. Aliaga, O. E. Martinez, G. B. Mindlin, and A. Lipsich, *Phys. Rev. Lett.* **83**, 292 (1999).
 - [15] J. F. Martinez-Avila, H. L. D. de S. Cavalcante, and J. R. Rios Leite, *Phys. Rev. Lett.* **93**, 144101 (2004).
 - [16] Y. Hong and K. Shore, *Opt. Lett.* **30**, 3332 (2005).
 - [17] Y. Hong and K. A. Shore, *IEEE J. Quantum Electron.* **41**, 1054 (2005).
 - [18] C. Masoller, *Chaos* **7**, 455 (1997).
 - [19] J. Mork, B. Tromborg, and J. Mark, *IEEE J. Quantum Electron.* **28**, 93 (1992).
 - [20] V. Ahlers, U. Parlitz, and W. Lauterborn, *Phys. Rev. E* **58**, 7208 (1998).
 - [21] J. Tiana-Alsina, M. C. Torrent, O. A. Rosso, C. Masoller, and J. Garcia-Ojalvo, *Phys. Rev. A* **82**, 013819 (2010).
 - [22] C. Bandt and B. Pompe, *Phys. Rev. Lett.* **88**, 174102 (2002).
 - [23] C. Bandt, G. Keller, and B. Pompe, *Nonlinearity* **15**, 1595 (2002).
 - [24] M. T. Martin, A. Plastino, and O. A. Rosso, *Physica A* **369**, 439 (2006).
 - [25] S. Jalan, J. Jost, and F. M. Atay, *Chaos* **16**, 033124 (2006).
 - [26] W. S. Lam, P. Guzdar, and R. Roy, *Int. J. Mod. Phys. B* **17**, 4123 (2003).
 - [27] J. Tiana-Alsina, J. M. Buldú, M. C. Torrent, and J. Garcia-Ojalvo, *Philos. Trans. R. Soc. London Ser. A* **368**, 367 (2010).
 - [28] E. A. Viktorov and P. Mandel, *Phys. Rev. Lett.* **85**, 3157 (2000).
 - [29] G. Huyet, P. A. Porta, S. P. Hegarty, J. G. McInerney, and F. Holland, *Opt. Commun.* **180**, 339 (2000).
 - [30] A. Prasad, Y. C. Lai, A. Gavrielides, and V. Kovanis, *J. Opt. B* **3**, 242 (2001).
 - [31] R. Lang and K. Kobayashi, *IEEE J. Quantum Electron.* **16**, 347 (1980).
 - [32] T. Heil, J. Mulet, I. Fischer, W. Elsasser, and C. R. Mirasso, *Opt. Lett.* **24**, 1275 (1999).
 - [33] D. W. Sukow, T. Heil, I. Fischer, A. Gavrielides, A. Hohl-AbiChedid, and W. Elsasser, *Phys. Rev. A* **60**, 667 (1999).
 - [34] J. M. Buldú, T. Heil, I. Fischer, M. C. Torrent, and J. Garcia-Ojalvo, *Phys. Rev. Lett.* **96**, 024102 (2006).

- [35] J. M. Mendez, R. Laje, M. Giudici, J. Aliaga, and G. B. Mindlin, [Phys. Rev. E **63**, 066218 \(2001\)](#).
- [36] J. M. Mendez, J. Aliaga, and G. B. Mindlin, [Phys. Rev. Lett. **89**, 160601 \(2002\)](#).
- [37] J. Zamora-Munt, C. Masoller, and J. García-Ojalvo, [Phys. Rev. A **81**, 033820 \(2010\)](#).
- [38] J. M. Mendez, J. Aliaga, and G. B. Mindlin, [Phys. Rev. E **71**, 026231 \(2005\)](#).